

3D-Printed Metal Surgical Guide for Endodontic Microsurgery (a Proof of Concept)

Camille Cabezon, Davy Aubeux, Fabienne Pérez  and Alexis Gaudin * 

Department of Endodontics and Restorative Dentistry of Nantes Dental School, Nantes Université, Oniris, CHU Nantes, INSERM, Regenerative Medicine and Skeleton, RMeS, F-44000 Nantes, France

* Correspondence: alexis.gaudin@univ-nantes.fr; Tel.: +33-6240412913

Featured Application: 3D-printed metal surgical guides offer several advantages (open-frame, stability) over traditional resin guides. This proof-of-concept study demonstrates the feasibility and the potential use of such guides during endodontic microsurgery procedures.

Abstract: Thanks to recent advances, printed surgical guides are now fully integrated into digital workflows and are beneficial in terms of accuracy in endodontic microsurgery (EMS). The aim of this study was to evaluate the accuracy of new 3D-printed surgical metal guides (SMGs) with open-frame structures in an endodontic surgical simulation model *ex vivo* based on a pig jaw. Twenty-nine roots were included. SMGs were produced using 3D implant planning software and printed using cobalt-chrome and a laser sintering printer. The SMGs were designed to allow for surgical access at 3 mm from the apex of each root. Virtual planning and postoperative CBCT scans were compared by analysing the apical and angular deviations. To test for deviations equal to zero, a one-sample test was used. The differences between the virtually planned implant and the actual position of the drill path were statistically significant for five SMGs on the eight produced guides, whereas there were no differences for the three others. The mean apical deviation was $3.2 \text{ mm} \pm 1.7$ using SMGs, and the angular deviation was measured at $3.10 \text{ degrees} \pm 2.37$. Although deviations were observed, the results demonstrate the feasibility and the potential for such guides during EMS procedures.

Keywords: apicoectomy; 3D-printed template; cone beam computed tomography; endodontics; guided surgery



Citation: Cabezon, C.; Aubeux, D.; Pérez, F.; Gaudin, A. 3D-Printed Metal Surgical Guide for Endodontic Microsurgery (a Proof of Concept). *Appl. Sci.* **2023**, *13*, 1031. <https://doi.org/10.3390/app13021031>

Academic Editor: Luca Testarelli

Received: 24 December 2022

Revised: 5 January 2023

Accepted: 10 January 2023

Published: 12 January 2023



Copyright: © 2023 by the authors. Licensee MDPI, Basel, Switzerland. This article is an open access article distributed under the terms and conditions of the Creative Commons Attribution (CC BY) license (<https://creativecommons.org/licenses/by/4.0/>).

1. Introduction

Endodontic microsurgery (EMS) is one of the treatment options for endodontically treated teeth with unresolved periapical lesions, anatomically complex roots, and cases of iatrogenic accidents. One major challenge during EMS is ensuring adequate visual and instrumental access to the root apex. This is especially important in scenarios in which lesions have not yet perforated the cortical plate.

Some studies have reported that tooth position has an influence on the success rate. In particular, the lower molars have been reported to have a lower success rate than other teeth due to their visual and instrumental access difficulties [1,2]. Other challenges include avoiding the risk of complications and iatrogenic problems such as pain, swelling, bleeding, and nerve injuries. When performing EMS, management of vital anatomic structures and the adjacent root apex is crucial (including the inferior alveolar nerve, sinus, nasal cavity, greater palatine artery, and mental foramen) [3]. Lastly, minimizing the size of the access window to the apex has been correlated with better healing outcomes [4].

To improve the accuracy during EMS, surgical guides have recently been introduced [5]. Surgical guides have traditionally been used in implantology since 2002 [6]. The placement of dental implants is more accurate and predictable when using a surgical guide with computer-aided design and computer-aided manufacturing (CAD-CAM)

technologies than freehand surgery [7–9]. Thanks to advances in technologies including stereolithography, optical scanning, cone beam computed tomography (CBCT), and 3D printing, surgical printed guides are now fully integrated in digital workflows and have become easy to produce [10–13].

Several case reports indicate that using 3D-printed surgical guides during EMS allows for more accurate surgical access without the risk of damaging vital structures [1,14,15]. All of these printed surgical guides are made of autoclavable, biocompatible resin. They cover the teeth and gums over the entire arch or half of the arch for stability [5,16]. Although transparent, such guides are made to be thick to compensate for fragility, which leads to visual disturbance and a need to insert a sleeve.

To overcome these drawbacks and facilitate the sterilization process and irrigation during surgery, surgical metal guides (SMGs) using cobalt-chrome with laser sintering have recently been designed and introduced in dental surgery [17]. The goal is to make guided surgery faster, easier, and more accurate [18–20]. Current concepts of removable partial dentures (RPDs) are focused on biomechanical aspects such as stability, retention, and mechanical resistance. To achieve these goals, RPDs are usually made with metal, and the current metal of choice is cobalt-chrome [21,22]. This metal offers several advantages, such as lightweight, solidity, and the possibility of performing guided surgery without a sleeve.

This study introduces a new 3D-printed cobalt-chrome SMG with open-frame structure that may be used for EMS. This SMG fits around teeth, and stability is primarily achieved with metal contacts between the teeth and the metal framework of the guide according to current concepts of RPDs. The application of such concepts to surgical guides is new, and to our knowledge, there are no published cases or studies evaluating this type of guide for EMS. Before considering its clinical use, its feasibility and accuracy must be assessed. The purpose of this study was to evaluate the accuracy of 3D-printed SMGs in comparison to virtual planning in an endodontic surgical simulation model *ex vivo* using a pig jaw. To assess the accuracy of the surgical guides, virtually planned implants were compared to bone drilled with SMGs in terms of apical and angular deviations. The main hypothesis was that there would be no significant statistical differences between virtually planned implants and drill paths after surgery. The resulting information is a first step in validating the accuracy of 3D-printed metal endodontic surgical guides.

2. Materials and Methods

2.1. Study Design

The study protocol was reviewed and approved by the Nantes School of dentistry (IR.NU.ENDO.01). The use of pig jaws followed the school's regulations. Mandibles were removed from the animals and cleaned in an abattoir according to our instructions. Only healthy samples with unimpaired teeth, gingival tissues, and alveolar mucosa were selected. The mandibles of pigs were used. In addition to crowns of teeth, two metallic screws were fixed in each mandible in order to serve as landmarks for matching optical scans and radiography. The total of 29 roots included: 4 roots for mandibles 1 to 6, 3 roots for mandible 7, and 2 roots for mandible 8. The number of roots selected depended on root proximities, technical feasibility for the guides, and distances from the landmark screws fixed in each mandible. The mandibles were maintained in a refrigerator with no fixatives. Prior to laboratory use, the frozen mandibles were maintained at room temperature until the tissues were soft and pliable. Figure 1 depicts the workflow diagram of the whole procedure from start to finish.

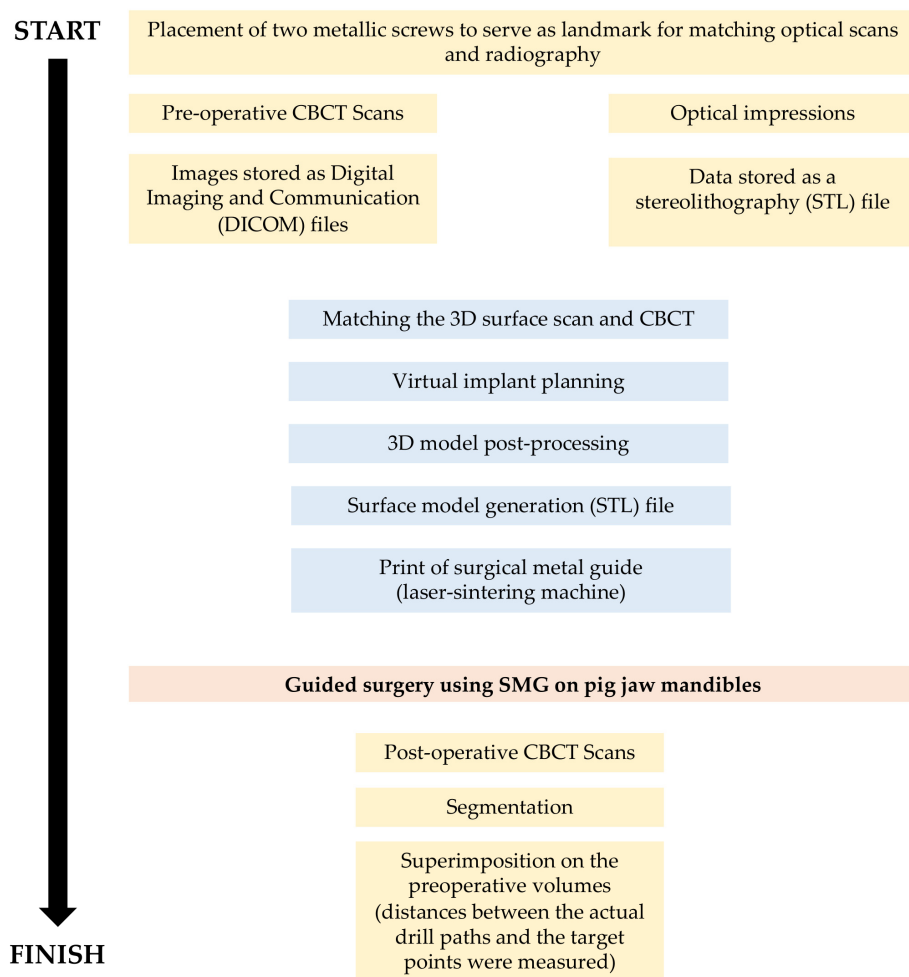


Figure 1. Workflow diagram of the study design.

2.2. Experimental Procedure

Preoperative CBCT scans of all jaws were obtained with an Orthophos XG 3D CBCT unit (Dentsply Sirona, York, Pennsylvania, USA) with an 8 cm × 8 cm field of view and a 0.16-mm voxel size. The parameters were 85 kV, 6 mA, and an exposure time of 14.2 s. Images were stored as Digital Imaging and Communication (DICOM) files. Optical impressions of the teeth were taken using a CARESTREAM CS3600 scanner (Carestream, New York, NY, USA), and data were stored as a stereolithography (STL) file. The datasets obtained from the digital workflow were uploaded to the 3D implant planning software 3Shape Implant Studio (3 Shape, Copenhagen, Denmark). The software was used to design a virtual template by matching the 3D surface scan and CBCT data while aligning the key points of the crowns of the teeth.

Virtual implant planning was performed by placing four virtual implants on each side of a pig jaw (STRAUMAN implant diameter 2.5 mm; length 12 mm or 10 mm depending on the situation). The target was the middle of each root at 3 mm above the apex. The virtual implants were inclined at the nearest angle of 80–90 degrees to the dental axis. The surgical guide was designed and fabricated by laser sintering using a 3D printer (Pro X DMP 200 dental, 3D systems, Riom, France; laboratory BONGERT, La Roche sur Yon, France). Depth control was achieved by adjusting the thickness of the guide so that when the surgical drill (length 17 mm, diameter 1.9 mm; ASTRA TECH, Implant System EV) was sunk into the head of the handpiece, it would access 3 mm from the apex of each root with control of the depth to the lingual surface of the root. SMGs were printed in cobalt-chrome, and the design followed current concepts of RPDs to increase stability (Figure 2a–c).

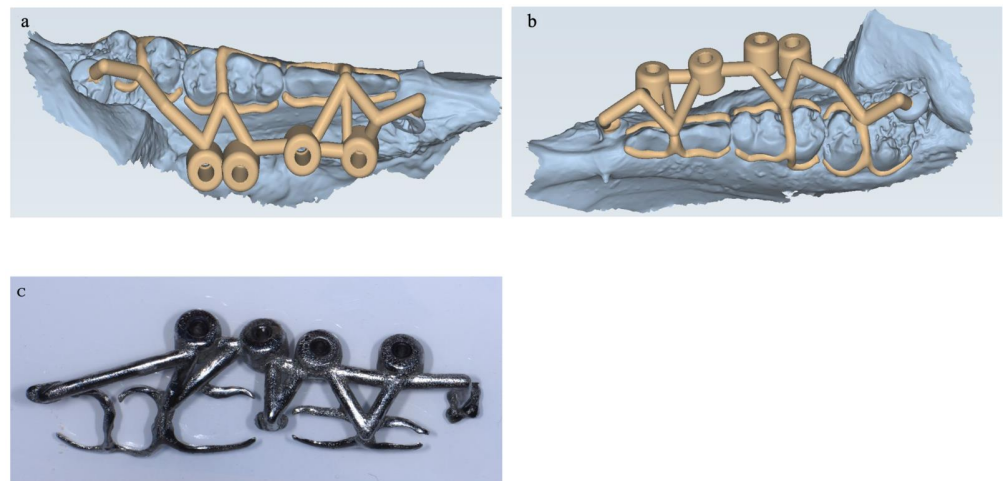


Figure 2. Planification of the 3D-printed surgical metal guide. Eight virtual surgical guides were designed using 3D implant planning software 3Shape Implant Studio. (a) Occluso-buccal and (b) occluso-lingual views showing one example of the virtual surgical guide in yellow and the optical scan of the mandible pig jaw in blue. (c) The different SMGs were 3D-printed in cobalt-chrome.

On the night before surgery, the bones were thawed slowly at 4 °C and then maintained at room temperature. The cheek muscles were retracted to improve visual and instrumental access. Using a sterile no. 15 blade, an intrasulcular incision was extended across 1–2 teeth mesially and distally from the study tooth. This was followed by a vertical release incision mesially. A full-thickness mucoperiosteal flap was then created to expose the bone, and the guides were placed over the occlusal surface of the teeth. Guided osteotomy was performed using a 1.9 mm-diameter, 17 mm-long drill and irrigated with water. The drill speed was 10,000 RPM, and the procedure was performed using a pecking motion until the drill stopped (Figure 3a–d).

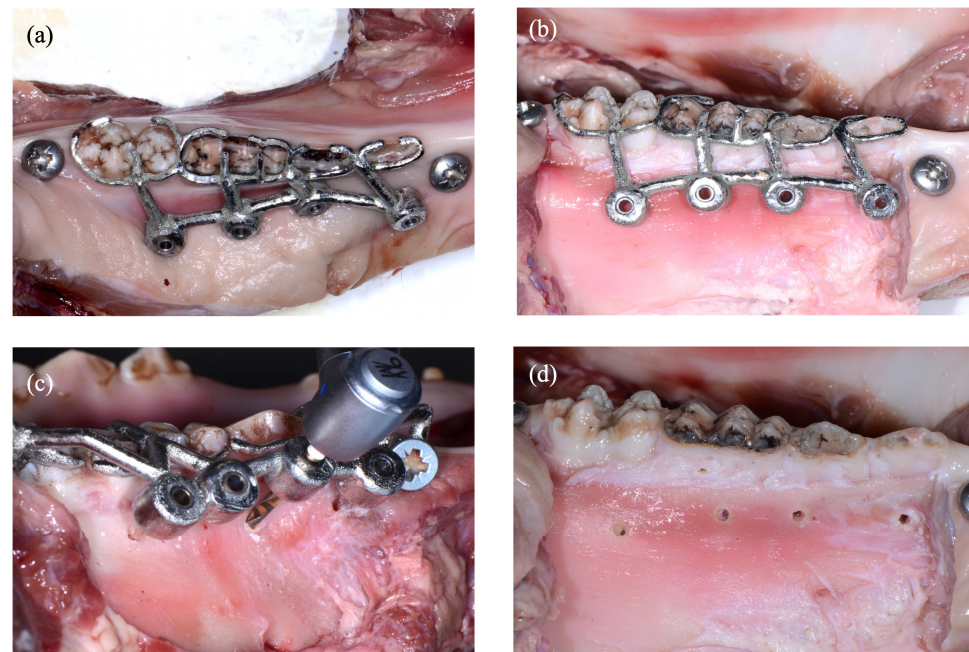


Figure 3. Guided surgery using SMG on pig jaw mandible. (a) The adjustment was checked in order to control the stability of the SMG. (b) After flap resection, the SMG was placed over the occlusal surface of the teeth. (c) The drill was driven through the metal sleeve until it reached the determined stop. (d) The final situation shows four drilled paths through the bone.

2.3. Measurement Procedure

After guided surgery, postoperative CBCT scans were taken of each side of the pig jaw with the same settings as the preoperative scans. Using the software BlueSkyPlan 4 (BlueSkyBio, Libertyville, IL, USA), the drill path was automatically segmented via a slice-by-slice method and transformed into a three-dimensional virtual model. As a next step, STL files of the drill path and initial planning were superimposed using 3Shape Implant Studio by aligning the crowns of each tooth. The CBCT analysis used a specific algorithm to minimize the relative distance according to an interactive process of the files matching, guaranteeing accurate and repeatable overlaying. Following the alignment process, a mean error value was calculated using the distance of the points between the two surfaces (from the STL and the DICOM files), which were considered acceptable when less than 0.1–0.15 mm.

To compare the result of the osteotomy with the plan in terms of the deviation of the principal axes, the deviation of each drill path created with the SMGs and initial planning was measured in 3 dimensions. To calculate the Euclidean distances, the following formula was used:

$$\sqrt{x^2 + y^2 + z^2}$$

where x , y , and z are the sagittal, coronal, and axial distances between the end of the drill path created with the SMGs and the end of the preplanned virtual implant, respectively (Figure 4a–e). The angular deviation was defined as the angle closed by the principal axes of the aligned models in degrees. All measurements were repeated three times.

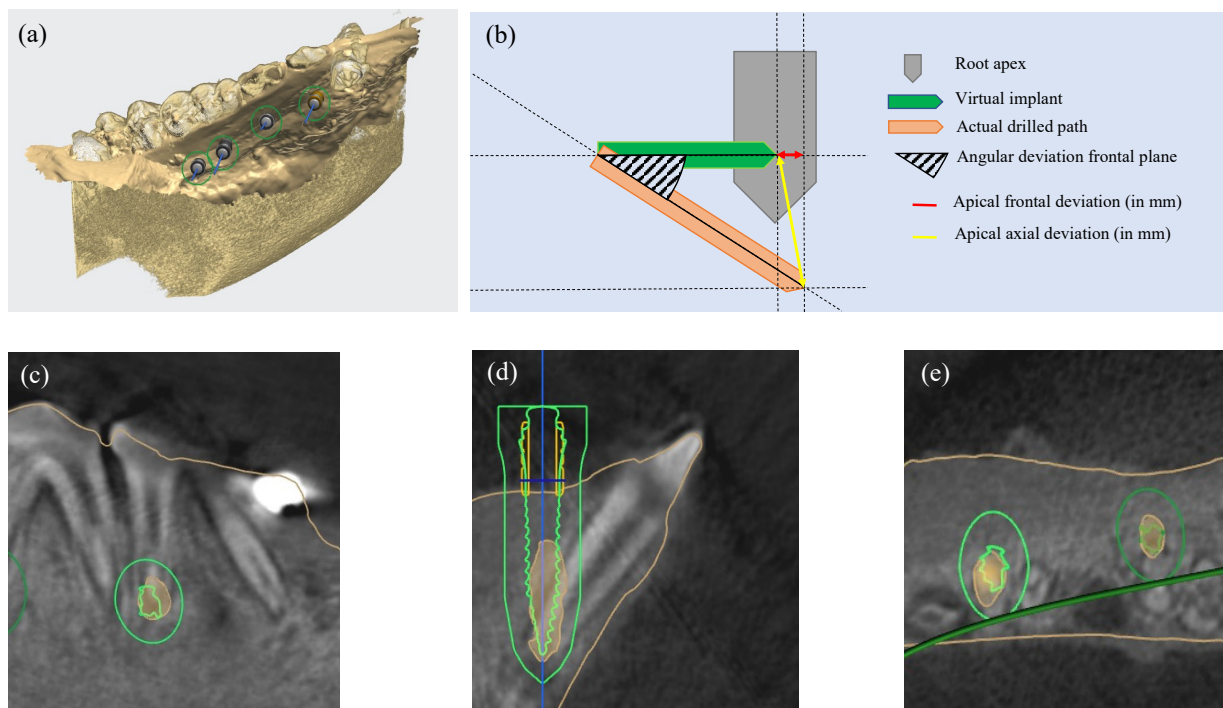


Figure 4. Determination of the measurement deviation calculation and angular deviation at the level of the apex. (a) The preoperative 3D reconstruction of the pig jaw shows the virtual implants in direction of the targeted root apices. (b) The illustration shows the calculation of the apical deviation of the tip of the virtual implant in comparison with the actual drilled path. (c) Sagittal view, (d) coronal view, and (e) axial view of the superposition between the virtual planned implant (green) and the actual drill path (orange). The green circle represents the implant's safety zone. The blue line shows the main axis of the implant. The dark green line represents the panoramic curve.

2.4. Statistical Analysis

Statistical calculations were performed using statistical software (GraphPad Prism, San Diego, CA, USA). To test for deviation equal to zero, a one-sample *t* test was used. Deviations were summarized using the mean, minimum, maximum, median, and standard deviation and the corresponding 95% confidence interval (CI). All tests were 2-sided, and *p* = 0.05 was considered statistically significant.

3. Results

A total of 29 implants were planned, and eight SMGs were printed. A summary of the deviation in each case is presented in Table 1. The mean differences between planned and actual positions of the drill path were significantly different for the outcome apical deviation (*p* < 0.05). The differences between the virtually planned implant and the actual position of the drill path were statistically significant for SMGs 1, 2, 3, 4, and 5, whereas there was no difference for SMGs 6, 7, and 8. The mean apical deviation was 3.2 mm ± 1.7 using SMGs.

Table 1. Statistic summary of the deviation between the planned and the actual paths for each of the 3D-printed surgical metal guides.

	n	Apical Deviation							<i>p</i>
		Mean	Min	Max	Median	SD	95% CI LL	95% CI UL	
SMG 1	4	2.38	1.55	3.11	2.43	0.77	1.55	3.11	0.0087
SMG 2	4	4.90	2.67	6.38	5.28	1.66	2.67	6.38	0.0097
SMG 3	4	4.24	2.46	6.58	3.95	1.72	2.46	6.58	0.016
SMG 4	4	4.85	3.8	5.67	4.97	0.92	3.08	5.67	0.0019
SMG 5	4	3.75	2.65	5.87	3.24	1.51	2.65	5.87	0.0156
SMG 6	4	1.25	0.77	2.56	0.83	0.87	0.77	2.56	0.0646
SMG 7	3	1.99	1.2	3.14	1.6	1.01	1.23	3.14	0.076
SMG 8	2	1.86	1.24	2.47	1.86	0.86	1.24	2.47	0.2025
Total	29	3.28	0.77	6.58	2.97	1.76	2.61	3.95	<0.001

The apical deviations between the preoperatively planned and actual drill paths are expressed with mean, minimum, maximum, median, and standard deviation for each 3D metal guide (in millimeters). SMG: 3D-printed surgical metal guides; n, number of virtual implant planned; min, minimum; max, maximum; med, median; SD, standard deviation; LL: lower level, UL: upper level.

The mean deviation in the sagittal plane was 1.59 ± 1.43 mm (median: 1.46, min: 0.33, max: 6.26; *t*(7) = 3.741, *p* = 0.0073). In the frontal plane, the mean deviation was 2.00 ± 1.28 mm (median: 1.93, min: 0.00, max: 5.10; *t*(7) = 5.902, *p* = 0.0006). In the axial plane, the mean deviation was 1.37 ± 1.15 (median: 0.90, min: 0.20, max: 4.30; *t*(7) = 4.114, *p* = 0.0045).

The angular deviation (in degrees) between the estimated and realized holes with the 3D-printed surgical guide was 3.10 degrees ± 2.37 (median: 2.79 min: 0.08, max: 10.69; *t*(7) = 6.824, *p* = 0.0002).

4. Discussion

Guided endodontic microsurgery is becoming recognized as more accurate than freehand surgery [5,16]. Guides evolve to best adapt to the clinical situation and are being improved with technical developments. The present study has proposed a new design for a printed SMG, and its accuracy was evaluated using a model *ex vivo*. Two parameters were assessed: the accuracy of the most apical point of the drill path and the angular deviation. These two parameters are often chosen in studies because they are easily identifiable and present reliable information concerning the assessment of the difference between the actual results and virtual planning.

The angular deviation is an important parameter because it determines the root-end resection and whether all of the accessory canals can be resected [23]. Using SMGs, the angular deviation was 3.1 ± 1.3 degrees. Data related to the angular deviation are very scarce. Only one study has reported an overall angulation of 3.95 degrees (95% CI: 2.1–5.9 degrees) using a trephination guide for endodontic surgery [14]. This result is in accordance with our results.

Of note, the angular deviation has been evaluated in multiple implantology studies. Pettersson et al. compared the deviation between the position of virtually planned implants and the position of implants placed with a printed surgical guide in a human cadaver [24]. The mean angular deviation of the mandible was 2.26 degrees (range: 0.24–11.74 degrees; 95% CI: 2.01). Younes et al. reported a mean angular deviation of 2.30 ± 0.92 degrees [7]. Benheke et al. analysed the factors influencing the accuracy of a printed surgical guide for implant placement and reported a mean angular deviation of 2.25 degrees (0.07–5.82 degrees) for the mandible [25].

The overall mean deviation between the most apical points planned and those performed with the surgical guide were superior to previous studies performed using human mandibles and resin guides. Pinsky et al. found a mean deviation of 0.79 ± 0.33 mm [5] and Ackerman et al. obtained a mean deviation of 1.47 ± 0.75 mm for the same parameters [16]. These results may be explained because of the variation between the different SMGs. Three out of eight of the different SMGs did not express any statistical difference between the most apical points planned and those performed with the surgical guide, whereas the others expressed quite high values. One explanation for the variation could be that several drill paths (up to four) were achieved with the same guide to maximize the number of roots in the study to be compared. Schelbert et al. observed that multiple implants placed with the same guide showed higher mean deviations than single implants [26]. This has also been observed by Widmann et al. in 2006 [27].

Previous studies have used preoperative and postoperative CBCT scan datasets to measure angular deviation [16,28]. However, a limitation exists in this protocol because all software has an internal error which is different from the real measurement. CBCT scan datasets may differ due to different orientations of objects. In our study, a specific guide was created to correctly position the jaws. A “scan body” of the implant placed in the drilled path could have been used to allow for the addition of scan datasets. However, this method requires the body scans to be stable in the drilled path. The distance measurements were manually calculated by two blinded observers (an endodontist and a general practitioner familiar with the software). Although this methodology was based on a preliminary study, this may have led to small errors in the calculations. The use of computer software to automatically calculate the deviation between planned and performed drill path by registering preoperative and postoperative CBCT scans may be relevant for future studies [29].

Nowadays, most guide systems are using resin 3D-printed surgical guides with metal sleeves for drill guidance. However, these resin 3D-printed surgical guides have some limitations. Common issues reported with surgical guides are lack of fit and stability, limited irrigation possibilities, and the lack of visibility due to the intrinsic volume of the guide [30,31]. Today, there are alternatives to this approach for 3D-printed surgical guides or guided surgery systems [17,32]. Thanks to the development of the relevant technology, in particular for partial denture removal due to a need to improve precision and the satisfaction of patients, the cost of such guides recently decreased to be comparable with resin guides. The advantage of the SMG is the open frame that allows visibility and irrigation while maintaining stability.

Interestingly, SMGs offer the advantage to potentially eliminate the sleeves. The presence of the sleeve, in fact, forces the surgeon to use long drills available only in surgical kits specifically dedicated to guided surgery. Tallarico et al. showed that surgical guides without metallic sleeves were more accurate than a conventional guide with a metallic sleeve [18]. Although sleeves were used in this study, one of the advantages of a metal guide is that it is possible to use it without a sleeve, thus avoiding this bias [17]. The next step will be to design, produce, and assess SMGs without sleeves.

This study was a proof of concept using a simple ex vivo model. Although the model did not fully replicate conditions in vivo (pig teeth are larger than human teeth and tooth shapes decrease the stability of the guide), this ex vivo model offers advantages. The bone density of a young pig jaw is similar to that of a human mandible [33]. According to Behneke et al., this is a crucial factor when assessing the accuracy of a surgical guide [25].

This simulation model is easy to handle and cost-effective, and different experiments may be performed (CBCT, histology) because repeated freeze-thaw cycles do not alter the bone [34].

5. Conclusions

To the best of our knowledge, this study is the first to consider the use of 3D-printed surgical metal guides from the perspective of EMS applications. Before translation to human therapy, further studies should be conducted to determine their predictability and to compare with traditional resin guides. This proof-of-concept study demonstrates its feasibility in an ex vivo model and suggests the potential for such guides during EMS procedures.

Author Contributions: Conceptualization, C.C. and A.G.; methodology, C.C. and A.G.; software, C.C.; validation, C.C. and A.G.; formal analysis, C.C.; writing—original draft preparation, C.C. and A.G.; writing—review and editing, D.A. and F.P.; visualization, F.P.; supervision, A.G.; project administration, F.P.; funding acquisition, F.P. All authors have read and agreed to the published version of the manuscript.

Funding: This study was supported by the Department of Endodontics and Restorative Dentistry of Nantes Dental School (GR 210979).

Institutional Review Board Statement: The study protocol was reviewed and approved by the Nantes School of Dentistry (IR.NU.ENDO.01; 7 January 2019).

Informed Consent Statement: Not applicable.

Data Availability Statement: Data sets used during the study are available from the corresponding author(s) on reasonable request.

Acknowledgments: This article is based on a resident in endodontics. We would like to thank Yannick Gourrier (Digital labs[®]) for printing the surgical metal guides. We would also like to thank Edouard Lanoiselée and Loïc Buffard for their helpful discussions. Finally, we would like to thank the Department of Endodontics and Restorative Dentistry for financial support.

Conflicts of Interest: The authors declare no conflict of interest.

References

1. Ahn, S.Y.; Kim, N.H.; Kim, S.; Karabucak, B.; Kim, E. Computer-Aided Design/Computer-Aided Manufacturing-Guided Endodontic Surgery: Guided Osteotomy and Apex Localization in a Mandibular Molar with a Thick Buccal Bone Plate. *J. Endod.* **2018**, *44*, 665–670. [[CrossRef](#)] [[PubMed](#)]
2. Hajihassani, N.; Ramezani, M.; Tofangchiha, M.; Bayereh, F.; Ranjbaran, M.; Zanza, A.; Reda, R.; Testarelli, L. Pattern of Endodontic Lesions of Maxillary and Mandibular Posterior Teeth: A Cone-Beam Computed Tomography Study. *J. Imaging* **2022**, *8*, 290. [[CrossRef](#)] [[PubMed](#)]
3. Reda, R.; Zanza, A.; Bhandi, S.; Biase, A.D.; Testarelli, L.; Miccoli, G. Surgical-Anatomical Evaluation of Mandibular Premolars by CBCT among the Italian Population. *Dent. Med. Probl.* **2022**, *59*, 209–216. [[CrossRef](#)] [[PubMed](#)]
4. Arx, T.V.; Hänni, S.; von Arx, T.; Hänni, S.; Jensen, S.S. Correlation of Bone Defect Dimensions with Healing Outcome One Year after Apical Surgery. *J. Endod.* **2007**, *33*, 1044–1048. [[CrossRef](#)]
5. Pinsky, H.M.; Champeboux, G.; Sarment, D.P. Periapical Surgery Using CAD/CAM Guidance: Preclinical Results. *J. Endod.* **2007**, *33*, 148–151. [[CrossRef](#)]
6. Sarment, D.P.; Sukovic, P.; Clinthorne, N. Accuracy of Implant Placement with a Stereolithographic Surgical Guide. *Int. J. Oral Maxillofac. Implant.* **2003**, *18*, 571–577.
7. Younes, F.; Cosyn, J.; De Bruyckere, T.; Cleymaet, R.; Bouckaert, E.; Eghbali, A. A Randomized Controlled Study on the Accuracy of Free-Handed, Pilot-Drill Guided and Fully Guided Implant Surgery in Partially Edentulous Patients. *J. Clin. Periodontol.* **2018**, *45*, 721–732. [[CrossRef](#)] [[PubMed](#)]
8. Kernén, F.; Benic, G.I.; Payer, M.; Schär, A.; Müller-Gerbl, M.; Filippi, A.; Kühl, S. Accuracy of Three-Dimensional Printed Templates for Guided Implant Placement Based on Matching a Surface Scan with CBCT. *Clin. Implant Dent. Relat. Res.* **2016**, *18*, 762–768. [[CrossRef](#)]
9. Schneider, D.; Marquardt, P.; Zwahlen, M.; Jung, R.E. A Systematic Review on the Accuracy and the Clinical Outcome of Computer-Guided Template-Based Implant Dentistry. *Clin. Oral Implants Res.* **2009**, *20*, 73–86. [[CrossRef](#)]
10. Dawood, A.; Marti, B.M.; Sauret-Jackson, V.; Darwood, A. 3D Printing in Dentistry. *Br. Dent. J.* **2015**, *219*, 521–529. [[CrossRef](#)]

11. van der Meer, W.J.; Vissink, A.; Ng, Y.L.; Gulabivala, K. 3D Computer Aided Treatment Planning in Endodontics. *J. Dent.* **2016**, *45*, 67–72. [[CrossRef](#)] [[PubMed](#)]
12. Oberoi, G.; Nitsch, S.; Edelmayer, M.; Janjić, K.; Müller, A.S.; Agis, H. 3D Printing—Encompassing the Facets of Dentistry. *Front. Bioeng. Biotechnol.* **2018**, *6*, 172. [[CrossRef](#)] [[PubMed](#)]
13. Ye, S.; Zhao, S.; Wang, W.; Jiang, Q.; Yang, X. A Novel Method for Periapical Microsurgery with the Aid of 3D Technology: A Case Report. *BMC Oral. Health* **2018**, *18*, 85. [[CrossRef](#)]
14. Antal, M.; Nagy, E.; Braunitzer, G.; Fráter, M.; Piffkó, J. Accuracy and Clinical Safety of Guided Root End Resection with a Trephine: A Case Series. *Head Face Med.* **2019**, *15*, 30. [[CrossRef](#)]
15. Giacomino, C.M.; Ray, J.J.; Wealleans, J.A. Targeted Endodontic Microsurgery: A Novel Approach to Anatomically Challenging Scenarios Using 3-Dimensional-Printed Guides and Trephine Burs—A Report of 3 Cases. *J. Endod.* **2018**, *44*, 671–677. [[CrossRef](#)] [[PubMed](#)]
16. Ackerman, S.; Aguilera, F.C.; Buie, J.M.; Glickman, G.N.; Umorin, M.; Wang, Q.; Jalali, P. Accuracy of 3-Dimensional-Printed Endodontic Surgical Guide: A Human Cadaver Study. *J. Endod.* **2019**, *45*, 615–618. [[CrossRef](#)]
17. Mouhyi, J.; Salama, M.A.; Mangano, F.G.; Mangano, C.; Margiani, B.; Admakin, O. A Novel Guided Surgery System with a Sleeveless Open Frame Structure: A Retrospective Clinical Study on 38 Partially Edentulous Patients with 1 Year of Follow-Up. *BMC Oral Health* **2019**, *19*, 253. [[CrossRef](#)]
18. Tallarico, M.; Martinolli, M.; Kim, Y.; Cocchi, F.; Meloni, S.M.; Alushi, A.; Xhanari, E. Accuracy of Computer-Assisted Template-Based Implant Placement Using Two Different Surgical Templates Designed with or without Metallic Sleeves: A Randomized Controlled Trial. *Dent. J.* **2019**, *7*, 41. [[CrossRef](#)]
19. Koop, R.; Vercruyssen, M.; Vermeulen, K.; Quirynen, M. Tolerance within the Sleeve Inserts of Different Surgical Guides for Guided Implant Surgery. *Clin. Oral Implants Res.* **2013**, *24*, 630–634. [[CrossRef](#)]
20. Anderson, J.; Wealleans, J.; Ray, J. Endodontic Applications of 3D Printing. *Int. Endod. J.* **2018**, *51*, 1005–1018. [[CrossRef](#)]
21. Tribst, J.P.M.; Dal Piva, A.M.D.O.; Borges, A.L.S.; Araújo, R.M.; da Silva, J.M.F.; Bottino, M.A.; Kleverlaan, C.J.; de Jager, N. Effect of Different Materials and Undercut on the Removal Force and Stress Distribution in Circumferential Clasps during Direct Retainer Action in Removable Partial Dentures. *Dent. Mater.* **2020**, *36*, 179–186. [[CrossRef](#)] [[PubMed](#)]
22. Lee, H.; Kwon, K.-R. A CAD-CAM Device for Preparing Guide Planes for Removable Partial Dentures: A Dental Technique. *J. Prosthet. Dent.* **2019**, *122*, 10–13. [[CrossRef](#)] [[PubMed](#)]
23. Kim, S.; Kratchman, S. Modern Endodontic Surgery Concepts and Practice: A Review. *J. Endod.* **2006**, *32*, 601–623. [[CrossRef](#)] [[PubMed](#)]
24. Pettersson, A.; Kero, T.; Gillot, L.; Cannas, B.; Fäldt, J.; Söderberg, R.; Näsström, K. Accuracy of CAD/CAM-Guided Surgical Template Implant Surgery on Human Cadavers: Part I. *J. Prosthet. Dent.* **2010**, *103*, 334–342. [[CrossRef](#)]
25. Behneke, A.; Burwinkel, M.; Behneke, N. Factors Influencing Transfer Accuracy of Cone Beam CT-Derived Template-Based Implant Placement. *Clin. Oral Implants Res.* **2012**, *23*, 416–423. [[CrossRef](#)] [[PubMed](#)]
26. Schelbert, T.; Gander, T.; Blumer, M.; Jung, R.; Rücker, M.; Rostetter, C. Accuracy of Computer-Guided Template-Based Implant Surgery: A Computed Tomography-Based Clinical Follow-up Study. *Implant. Dent.* **2019**, *28*, 556–563. [[CrossRef](#)]
27. Widmann, G.; Bale, R.J. Accuracy in Computer-Aided Implant Surgery—A Review. *Int. J. Oral Maxillofac. Implant.* **2006**, *21*, 305–313.
28. Fan, Y.; Glickman, G.N.; Umorin, M.; Nair, M.K.; Jalali, P. A Novel Prefabricated Grid for Guided Endodontic Microsurgery. *J. Endod.* **2019**, *45*, 606–610. [[CrossRef](#)]
29. Moreno-Rabié, C.; Torres, A.; Lambrechts, P.; Jacobs, R. Clinical Applications, Accuracy and Limitations of Guided Endodontics: A Systematic Review. *Int. Endod. J.* **2020**, *53*, 214–231. [[CrossRef](#)]
30. Hay, S.I.; Abajobir, A.A.; Abate, K.H.; Abbafati, C.; Abbas, K.M.; Abd-Allah, F.; Abdulle, A.M.; Abebo, T.A.; Abera, S.F.; Aboyans, V.; et al. Global, Regional, and National Disability-Adjusted Life-Years (DALYs) for 333 Diseases and Injuries and Healthy Life Expectancy (HALE) for 195 Countries and Territories, 1990–2016: A Systematic Analysis for the Global Burden of Disease Study 2016. *Lancet* **2017**, *390*, 1260–1344. [[CrossRef](#)]
31. Apostolakis, D.; Kourakis, G. CAD/CAM Implant Surgical Guides: Maximum Errors in Implant Positioning Attributable to the Properties of the Metal Sleeve/Osteotomy Drill Combination. *Int. J. Implant Dent.* **2018**, *4*, 34. [[CrossRef](#)] [[PubMed](#)]
32. Oh, K.C.; Park, J.M.; Shim, J.S.; Kim, J.H.; Kim, J.E.; Kim, J.H. Assessment of Metal Sleeve-Free 3D-Printed Implant Surgical Guides. *Dent. Mater.* **2019**, *35*, 468–476. [[CrossRef](#)]
33. Dahiya, K.; Kumar, N.; Bajaj, P.; Sharma, A.; Sikka, R.; Dahiya, S. Qualitative Assessment of Reliability of Cone-Beam Computed Tomography in Evaluating Bone Density at Posterior Mandibular Implant Site. *J. Contemp. Dent. Pract.* **2018**, *19*, 426–430. [[CrossRef](#)] [[PubMed](#)]
34. Shaw, J.M.; Hunter, S.A.; Gayton, J.C.; Boivin, G.P.; Prayson, M.J. Repeated Freeze-Thaw Cycles Do Not Alter the Biomechanical Properties of Fibular Allograft Bone. *Clin. Orthop. Relat. Res.* **2012**, *470*, 937–943. [[CrossRef](#)] [[PubMed](#)]

Disclaimer/Publisher’s Note: The statements, opinions and data contained in all publications are solely those of the individual author(s) and contributor(s) and not of MDPI and/or the editor(s). MDPI and/or the editor(s) disclaim responsibility for any injury to people or property resulting from any ideas, methods, instructions or products referred to in the content.